

# Quasinormal modes in time-dependent black hole background

Cheng-Gang Shao, Bin Wang\*

*Department of Physics, Fudan University,  
Shanghai 200433, People's Republic of China*

Elcio Abdalla†

*Instituto de Fisica, Universidade de Sao Paulo,  
C.P.66.318, CEP 05315-970, Sao Paulo, Brazil*

Ru-Keng Su‡

*China Center of Advanced Science and Technology (World Laboratory),  
P.B.Box 8730, Beijing 100080, People's Republic of China  
Department of Physics, Fudan University,  
Shanghai 200433, People's Republic of China*

## Abstract

We have studied the evolution of the massless scalar field propagating in time-dependent charged Vaidya black hole background. A generalized tortoise coordinate transformation were used to study the evolution of the massless scalar field. It is shown that, for the slowest damped quasinormal modes, the approximate formulae in stationary Reissner-Nordström black hole turn out to be a reasonable prescription, showing that results from quasinormal mode analysis are rather robust.

PACS numbers: 04.30-w,04.62.+v

---

\*Electronic address: binwang@fudan.ac.cn

†Electronic address: eabdalla@fma.if.usp.br

‡Electronic address: rksu@fudan.ac.cn

## I. INTRODUCTION

It is well known that the surrounding geometry of a black hole will experience damped oscillations under perturbations. These oscillations are called "quasinormal modes" (QNM), which is believed to be a characteristic "sound" of black holes, and would lead to the direct identification of the black hole existence through gravitational wave observation, to be realized in the near future. In the past few decades, a great deal of effort has been devoted to the study of QNMs of black holes in asymptotically flat spacetimes (for comprehensive reviews see [1,2] and references therein). Considering the case when the black hole is immersed in an expanding universe, the QNMs of black holes in de Sitter space have also been investigated [3-5]. Motivated by the recent discovery of the Anti-de Sitter/Conformal Field Theory (AdS/CFT) correspondence, many authors have performed the study of QNMs in AdS spaces [6-18]. The study of the QNMs plays an important role in astrophysics, black hole physics and also string theory.

All these previous works on QNMs have so far been restricted to time-independent black hole backgrounds. It should be realized that, for a realistic model, the black hole parameters change with time. A black hole gaining or losing mass via absorption (merging) or evaporation is a good example. The more intriguing investigation of the black hole QNM calls for a systematic analysis of time-dependent spacetimes. Recently the late time tails under the influence of a time-dependent scattering potential has been explored in [19], where the tail structure was found to be modified due to the temporal dependence of the potential. The motivation of our work is to explore the modification to the QNM in time-dependent spacetimes. Instead of plotting an effective time-dependent scattering potential by hand as done in [19], we will introduce the time-dependent potential in a natural way by considering dynamical black holes, with black hole parameters changing with time due to absorption and evaporation processes. We will study the temporal evolution of massless scalar field perturbation. Instead of employing Kruskal-like coordinate in our first attempt before [20], here we start our discussion directly from the Vaidya metric.

The outline of this paper is as follows. In Sec. II we first go over the conventional treatment for the study of the wave propagation in stationary Reissner-Nordström (RN) black hole. In Sec. III, we will present the numerical way for the study of the QNMs of charged Vaidya black hole. We will present our numerical results in Sec. IV. Sec. V contains a brief summary and a discussion.

## II. QUASINORMAL MODES OF A STATIONARY REISSNER-NORDSTRÖM BLACK HOLE

Perturbation outside the stationary RN black hole has been discussed by many authors [21]. Here we first present a brief review on the conventional treatment of the evolution of massless scalar field propagating in RN black hole background.

The metric of a RN black hole in the ingoing Eddington coordinates is given by

$$ds^2 = -(1 - 2M/r + Q^2/r^2)dv^2 + 2dvdr + r^2(d\theta^2 + \sin^2\theta d\varphi^2) \equiv g_{\mu\nu}dx^\mu dx^\nu, \quad (1)$$

where  $v$  is a coordinate usually called the ‘advanced time’, which parameterizes a lapse of time. The propagation of scalar waves in curved spacetimes is governed by the Klein-Gordon equation

$$\partial_\mu(\sqrt{-g}g^{\mu\nu}\partial_\nu)\Phi = 0. \quad (2)$$

Since the background is spherically symmetric, each multipole of the perturbing field evolves separately. Hence one can define

$$\Phi = \sum_{l,m} \Psi(r, v) Y_{lm}(\theta, \varphi)/r. \quad (3)$$

Using the tortoise coordinate  $r_*$  defined by

$$r_* = r + \frac{r_+^2}{r_+ - r_-} \ln(r - r_+) - \frac{r_-^2}{r_+ - r_-} \ln(r - r_-), \quad (4)$$

where,  $r_+ = M + \sqrt{M^2 - Q^2}$  and  $r_- = M - \sqrt{M^2 - Q^2}$  are the radius of outer and inner horizons of the black hole, the wave equation for each multipole moment becomes

$$\Psi_{,r_*r_*} + 2\Psi_{,r_*v} - V\Psi = 0, \quad (5)$$

where

$$V(r_*) = \left(1 - \frac{2M}{r} + \frac{Q^2}{r^2}\right) \left(\frac{l(l+1)}{r^2} + \frac{2M}{r^3} - \frac{2Q^2}{r^4}\right). \quad (6)$$

Using the null coordinate

$$u = v - 2r_* \quad (7)$$

equation (5) can be written as

$$\Psi_{,uv} + \frac{1}{4}V\Psi = 0. \quad (8)$$

The two-dimensional wave equation (8) can be integrated numerically, using for example the finite difference method suggested in [22]. Using Taylor's theorem, it is discretized as

$$\Psi_N = \Psi_E + \Psi_W - \Psi_S - \delta u \delta v V \left( \frac{v_N + v_W - u_N - u_E}{4} \right) \frac{\Psi_W + \Psi_E}{8} + O(\varepsilon^4), \quad (9)$$

where the points  $N, S, E$  and  $W$  form a null rectangle with relative positions as:  $N : (u + \delta u, v + \delta v), W : (u + \delta u, v), E : (u, v + \delta v)$  and  $S : (u, v)$ . The parameter  $\varepsilon$  is an overall grid scalar factor, so that  $\delta u \sim \delta v \sim \varepsilon$ . For an RN black hole in de Sitter space this has been performed in [4].

In addition to solving (8) directly by numerical method, other ways have been suggested in studying the QNMs of RN black hole. For the slowest damped QNMs, the WKB formulas suggest the approximate behavior in RN black hole [23]

$$\begin{aligned} \omega_R &\approx (l + \frac{1}{2}) \left[ \frac{M}{r_0^3} - \frac{Q^2}{r_0^4} \right]^{1/2}, \\ \omega_I &\approx -\frac{1}{2} \left[ \frac{M}{r_0^3} - \frac{Q^2}{r_0^4} \right]^{1/2} \left[ 2 - 3 \frac{M}{r_0} \right]^{1/2}, \end{aligned} \quad (10)$$

in the limit  $l \gg 1$ . Here  $r_0 = \frac{3}{2}M + \frac{1}{2}(9M^2 - 8Q^2)^{1/2}$  is the position where the potential  $V$  attains its maximum value. Defining  $q = Q/M$ , the above equation becomes

$$\begin{aligned} M\omega_R &\approx c_R(l, q) \equiv (l + \frac{1}{2}) \left[ \frac{3}{2}(1 + \sqrt{1 - \frac{8}{9}q^2}) - q^2 \right]^{1/2} \left[ \frac{9}{2} - 2q^2 + \frac{9}{2}\sqrt{1 - \frac{8}{9}q^2} \right]^{-1}, \\ M\omega_I &\approx c_I(l, q) \equiv -\frac{3}{2} \left[ \frac{3}{2}(1 + \sqrt{1 - \frac{8}{9}q^2}) - q^2 \right]^{1/2} \left[ \frac{3}{2}(1 + \sqrt{1 - \frac{8}{9}q^2}) \right]^{-3} \sqrt{1 - \frac{8}{9}q^2}. \end{aligned} \quad (11)$$

The WKB computation has also been performed in the RN de Sitter Spacetime [4].

These conventional treatments are powerful in studying the wave propagation in stationary black hole background, however it is difficult to extend it to the time-dependent case. For the charged Vaidya black hole, the mass and the charge are functions of time,  $M = M(v), Q = Q(v)$ , and the standard tortoise coordinate can not be used to simplify the wave equation.

### III. FIELD EVOLUTION IN CHARGED VAIDYA BACKGROUND

The metric of the charged Vaidya spacetime reads

$$ds^2 = -\left(1 - \frac{2M(v)}{r} + \frac{Q^2(v)}{r^2}\right)dv^2 + 2cdvdr + r^2(d\theta^2 + \sin^2\theta d\varphi^2), \quad (12)$$

where  $M = M(v)$  and  $Q = Q(v)$  are arbitrary functions of the time. For  $c = 1$  the field is ingoing and  $M$  is monotone increasing in  $v$  (advanced time), and for  $c = -1$ , the field is outgoing and  $M$  is monotone decreasing in  $v$  (retarded time) [24]. The QNMs of a black hole correspond to the solutions of the Klein-Gordon equation that satisfy the causal condition that no information could

leak out through the event horizon of the black hole and at the same time correspond to purely outgoing waves at spatial infinity. For the charged Vaidya black hole, horizons  $r_{\pm}$  can be inferred from the null hypersurface condition  $g^{\mu\nu} f_{,\mu} f_{,\nu} = 0$  and  $f(r_{\pm}, v) = 0$ .  $r_{\pm}(v)$  satisfies the equation

$$r_{\pm}^2 - 2r_{\pm}M + Q^2 - 2cr_{\pm}^2\dot{r}_{\pm} = 0, \quad (13)$$

where  $\dot{r}_{\pm} \equiv dr_{\pm}/dv$ .

Since the charged Vaidya metric is spherically symmetric, a generalized tortoise coordinate transformation can be introduced as

$$r_* = r + \frac{1}{2k_+} \ln(r - r_+) - \frac{1}{2k_-} \ln(r - r_-), v_* = v - v_0, \quad (14)$$

which is similar to equation (4), and which we take as a simplifying Ansatz for our numerical equations upon an appropriated choice of the constants  $k_{\pm}$ , as well as the functions  $r_{\pm}(v)$ , which will be interpreted as the event and Cauchy horizons [27],  $r_+ = M + \sqrt{M^2 - Q^2 + 2cr_+^2\dot{r}_+}$  and  $r_- = M - \sqrt{M^2 - Q^2 + 2cr_-^2\dot{r}_-}$ , respectively. We take  $k_+$  and  $k_-$  as adjustable parameters to be defined. The parameter  $v_0$  is an arbitrary constant assumed to be zero now. From formulas (14) and (12), the Klein-Gordon equation for each multipole moment becomes

$$(1 + \varepsilon_2)\Psi_{,r_*r_*} + 2c\Psi_{,r_*v_*} + \varepsilon_1\Psi_{,r_*} - V\Psi = 0, \quad (15)$$

where

$$\varepsilon_2 = \frac{1}{r} \left( \frac{1 - 2c\dot{r}_+}{2k_+} - \frac{1 - 2c\dot{r}_-}{2k_-} - 2M \right) + \frac{1}{r^2} \left( \frac{(1 - 2c\dot{r}_+)r_+ - 2M}{2k_+} - \frac{(1 - 2c\dot{r}_-)r_- - 2M}{2k_-} + Q^2 \right),$$

$$\varepsilon_1 = A \left( \frac{1}{r^2} \left( \frac{1 - 2c\dot{r}_+}{2k_+} - \frac{1 - 2c\dot{r}_-}{2k_-} - 2M \right) - \frac{2\varepsilon_2}{r} \right),$$

$$V = A \frac{l(l+1)}{r^2} + A^2 \left( \frac{1}{r^3} \left( \frac{1 - 2c\dot{r}_+}{2k_+} - \frac{1 - 2c\dot{r}_-}{2k_-} - 2M \right) - \frac{2\varepsilon_2}{r^2} \right) - 2cA^2 \frac{1}{r} \left( \frac{\dot{r}_+}{2k_+(r-r_+)^2} - \frac{\dot{r}_-}{2k_-(r-r_-)^2} \right) + 2A^3 \frac{1}{r} \left( \frac{1}{2k_+(r-r_+)^2} - \frac{1}{2k_-(r-r_-)^2} \right) \left( \frac{c\dot{r}_+}{2k_+(r-r_+)} - \frac{c\dot{r}_-}{2k_-(r-r_-)} + \frac{1+\varepsilon_2}{2} \right), \quad (16)$$

with

$$A = \left( 1 + \frac{1}{2k_+(r-r_+)} - \frac{1}{2k_-(r-r_-)} \right)^{-1}.$$

For the convenience of numerical calculation, the adjustable parameters  $k_+$  and  $k_-$  can be selected in such a way that the Klein-Gordon equation for each multipole moment becomes the

standard wave equation near the horizons  $r_+(v_0)$  and  $r_-(v_0)$ . We define  $k_+$  and  $k_-$  by the algebraic equations

$$\begin{aligned}\frac{r_- - M - 2cr_- \dot{r}_-}{r_-^2} \frac{1}{k_-} - c \frac{\dot{r}_+ - \dot{r}_-}{r_+ - r_-} \frac{1}{k_+} &= -1 + 2c\dot{r}_-, \\ \frac{r_+ - M - 2cr_+ \dot{r}_+}{r_+^2} \frac{1}{k_+} - c \frac{\dot{r}_+ - \dot{r}_-}{r_+ - r_-} \frac{1}{k_-} &= 1 - 2c\dot{r}_+, \end{aligned}\tag{17}$$

at  $v = v_0$ . We impose for simplicity, that

$$\begin{aligned}\lim_{\substack{r \rightarrow r_{\pm}(v_0) \\ v \rightarrow v_0}} \varepsilon_2 &= \lim_{\substack{r \rightarrow r_{\pm}(v_0) \\ v \rightarrow v_0}} \varepsilon_1 = \lim_{v \rightarrow v_0} V = 0. \end{aligned}\tag{18}$$

For the static black hole with  $\dot{r}_+ = \dot{r}_- = 0$  (or  $M$  and  $Q$  are constants), we have the usual result  $\frac{1}{2k_{\pm}} = \frac{r_{\pm}^2}{r_+ - r_-}$ , when (14) boils down to (4) and (15) to (5).

Analogous to the coordinate used in (4), we make the variable transformation

$$u = u(r_*, v_*), v = v_*\tag{19}$$

where, the curve  $u(r_*, v_*) = \text{constant}$  is determined by the equation

$$\frac{dr_*}{dv_*} = \frac{1 + \varepsilon_2}{2c}.\tag{20}$$

For  $\varepsilon_2 \rightarrow 0$  and  $c = 1$ , we have  $u \rightarrow v_* - 2r_*$ , which is similar to (7). Using the transformation (19), equation (15) can be simplified to

$$\Psi_{,uv} - (2c \frac{\partial u}{\partial r_*})^{-1} V \Psi = 0.\tag{21}$$

The function  $u(r_*, v_*)$  can be integrated numerically according to equation (20). The integration of  $\Psi$  can proceed similarly to equation (9).

However, the numerical calculation discussed above has some difficulty for small  $Q$ , especially for the Vaidya metric with  $Q \rightarrow 0$ . In this case the inner horizon  $r_-$  disappears and the transformation (14) is no longer valid. In this case (14) can be replaced by [25]

$$r_* = r + \frac{1}{2k} \ln(r - r_+), \quad v_* = v - v_0\tag{22}$$

where  $k$  is an adjustable parameter. Using (22), the Klein-Gordon equation for each multipole moment has the same form as equation (15), only replacing the expressions of  $\varepsilon_2$ ,  $\varepsilon_1$  and  $V$  by

$$\varepsilon_2 = [2k(Q^2 - 2Mr) + r + r_+ - 2M - 2c(r + r_+)\dot{r}_+]/(2kr^2),$$

$$\varepsilon_1 = \frac{2k(r - r_+)}{2k(r - r_+) + 1} \left( \frac{1 - 2c\dot{r}_+ - 4kM}{2kr^2} - \frac{2\varepsilon_2}{r} \right),$$

$$V = \frac{2k(r - r_+)}{2k(r - r_+) + 1} \left( \frac{\varepsilon_1}{r} + \frac{2k(1 - 2c\dot{r}_+) + 2k\varepsilon_2}{(2k(r - r_+) + 1)^2 r} + \frac{l(l + 1)}{r^2} \right). \quad (23)$$

The parameter  $k$  can be selected to simplify the Klein-Gordon equation. We choose it such that

$$\begin{aligned} \lim_{\substack{r \rightarrow r_+(v_0) \\ v \rightarrow v_0}} \varepsilon_2 &= \lim_{\substack{r \rightarrow r_+(v_0) \\ v \rightarrow v_0}} \varepsilon_1 = \lim_{\substack{r \rightarrow r_+(v_0) \\ v \rightarrow v_0}} V = 0, \end{aligned} \quad (24)$$

namely

$$k = \frac{r_+(v_0)M(v_0) - Q(v_0)^2}{[2r_+(v_0)M(v_0) - Q(v_0)^2]r_+(v_0)}. \quad (25)$$

In the numerical calculation for the field evolution  $\Psi$ , the coordinate transformation (22) can be appropriated for  $Q \rightarrow 0$ .

In the following numerical calculation for the field  $\Psi$ , we always use a  $\delta$  pulse as an initial perturbation, located at  $v_0 = 0, r = 3$ . We first use our numerical method to the case of stationary RN black hole. The numerical result is in agreement with equation (10) or (11), even for  $l=2$ . Table 1 shows the slowest damped quasinormal frequencies for the scalar perturbation in the RN background with the multipole index  $l = 2$ . The numerical result is also in agreement with Ref. [4] for  $q=0$ .

Table I: The numerical result for  $M\omega_R$  (or  $M\omega_I$ ) and the lowest WKB approximate formulas for  $c_R(2, q)$  (or  $c_I(2, q)$ ) in the slowest damped quasinormal frequencies in the RN background. The multipole index  $l = 2$ .

| q     | $M\omega_R$ | $c_R(2, q)$ | $M\omega_I$ | $c_I(2, q)$ | $M\omega_R$ [4] | $M\omega_I$ [4] |
|-------|-------------|-------------|-------------|-------------|-----------------|-----------------|
| 0     | 0.483       | 0.481       | -0.0965     | -0.0962     | 0.484           | -0.0965         |
| 0.7   | 0.532       | 0.530       | -0.0985     | -0.0981     |                 |                 |
| 0.999 | 0.626       | 0.624       | -0.0889     | -0.0886     |                 |                 |

#### IV. NUMERICAL RESULT OF QNMS IN THE CHARGED VAIDYA BLACK HOLE

It is widely believed today that asymptotically flat black holes eventually evaporate due to the emission of Hawking radiation. For a RN black hole, we assume that at a certain retarded

moment  $v = v_0$  a charged nullfluid of negative-energy-density starts falling into the black hole (corresponding to the beginning of the evaporation process). We first adopt the ‘linear model’ [26], where  $M$  and  $Q$  depend linearly on  $v$ , and we also assume that the charge to mass ratio remains fixed.

$$M(v) = \begin{cases} m_0 & v \leq v_0 \\ m_0(1 - \lambda v) & v_0 \leq v \leq v_1 \\ m_1 & v \geq v_1 \end{cases} \quad (26)$$

$$Q(v) = qM(v),$$

where  $m_0$ ,  $m_1$ ,  $\lambda$  and  $q$  are constant parameters. The above model is initially a RN black hole for  $v < v_0$ . The evaporation process is displayed in the region  $v_0 < v < v_1$ . At  $v = v_1$ , the evaporation process stops, and the final geometry  $v > v_1$  is again the RN black hole. Changing the sign before  $\lambda$  in (26), this model can mimic the black hole absorption process. In the numerical study, we only consider how does the absorption or evaporation process affect the QNMs of the black hole in the region  $v_0 < v < v_1$ .

For the linear model (26), we can get the solution  $r_{\pm}$  of equation (13) as

$$\begin{aligned} r_+ &= M + M\sqrt{1 - q^2} & v > v_1, \\ r_+ &= \frac{M + M\sqrt{1 - q^2(1 - 2\dot{r}_+)}}{1 - 2\dot{r}_+}, & v \leq v_1, \\ r_- &= \frac{M - M\sqrt{1 - q^2(1 - 2\dot{r}_+)}}{1 - 2\dot{r}_+}, & v \geq v_0, \\ r_- &= M - M\sqrt{1 - q^2} & v < v_0, \end{aligned} \quad (27)$$

for absorption process with  $c = 1$ , and

$$\begin{aligned} r_+ &= \frac{M + M\sqrt{1 - q^2(1 + 2\dot{r}_+)}}{1 + 2\dot{r}_+}, & v \geq v_0, \\ r_+ &= M + M\sqrt{1 - q^2} & v < v_0, \\ r_- &= M - M\sqrt{1 - q^2} & v > v_1, \\ r_- &= \frac{M - M\sqrt{1 - q^2(1 + 2\dot{r}_+)}}{1 + 2\dot{r}_+}, & v \leq v_1, \end{aligned} \quad (28)$$

for evaporation process with  $c = -1$ . In general we suppose that  $|\dot{M}| = \lambda m_0 \ll 1$ , which leads to  $r_{\pm} \approx M \pm M\sqrt{1 - q^2}$ . Thus the  $r_+$  is very close to the outer apparent horizon  $M + M\sqrt{1 - q^2}$  [26], while the location of the  $r_-$  is very close to the inner apparent horizon  $M - M\sqrt{1 - q^2}$ . If  $q \rightarrow 1$ , then  $r_+ \approx M$ ,  $\dot{r}_+ \approx \dot{M}$ . Meanwhile equations (27) and (28) require  $1 - q^2(1 - 2c\dot{r}_+) \geq 0$ , which is obviously satisfied for both the absorption and evaporation cases. As an example, we take  $m_0 = 0.5$ ,  $\lambda = 0.002$ ,  $v_0 = 0$ ,  $v_1 = 150$  (correspondingly,  $m_1 = 0.35$  and  $\dot{M} = -0.001$ ). In Fig.1 we show behaviors of  $r_+$  and  $r_-$  for three different  $q$  in the evaporation process.

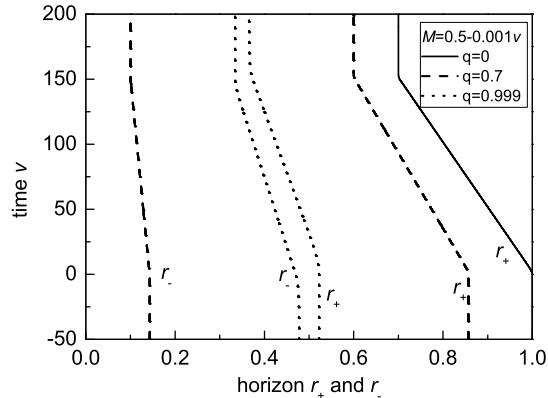


Figure 1: The behavior of  $r_+$  and  $r_-$  for the black hole with  $q=0$ ,  $q=0.7$  and  $q=0.999$ , respectively. The linear model is used with  $m_0 = 0.5$ ,  $\lambda = 0.002$ ,  $v_0 = 0$ ,  $v_1 = 150$  (correspondingly,  $m_1 = 0.35$  and  $\dot{M} = -0.001$ ).

The model (26) can represent the absorption process of the black hole when  $\lambda < 0$  (or  $m_0 < m_1$ ). As an example, the temporal evolution of the field  $\Psi$  in the Vaidya metric ( $q=0$ ) at  $r = 5$  is displayed in Fig.2. The relevant parameters were chosen as  $m_0 = 0.5$ ,  $\lambda = \pm 0.002$ ,  $v_0 = 0, v_1 = 150$ ,  $l = 2$ . The initial  $\delta$  pulse perturbation is located at  $v_0 = 0, r = 3$ . For comparison, we also exhibit the curve obtained for Schwarzschild black hole (replacing the time-dependent mass by a constant mass  $M = 0.5$ ). The modification to the QNMs due to the time-dependent background is clear. When  $M$  increases linearly with  $v$ , the decay becomes slower compared to the stationary case, which corresponds to saying that  $|\omega_I|$  decreases with respect to  $v$ . The oscillation period is no longer a constant as in the stationary Schwarzschild black hole. It becomes longer with the increase of time. In other words, the real part of the quasinormal frequency  $\omega_R$  decreases with the increase of time. When  $M$  decreases linearly with respect to  $v$ , compared to the stationary Schwarzschild black hole, we have observed that the decay becomes faster and the oscillation period becomes shorter, thus both  $|\omega_I|$  and  $\omega_R$  increase with time.

Next, we examine the behavior of the QNMs with the increase of the charge. The Figs. 3-6 display the frequency  $\omega_R$  and  $\omega_I$  as a function of  $v$  for  $l = 2$ , evaluated at  $r = 5$ . The mass of the black hole is  $M(v) = 0.5 \pm 0.001v$ . Both  $\omega_R$  and  $\omega_I$  can be determined. Different from the stationary case, all curves of  $\omega_R$  and  $\omega_I$  for different  $q$  increase or decrease linearly with respect to  $v$ . In general, as  $q$  increases from 0 to 1,  $\omega_R$  increases for different  $v$ .  $\omega_I$  exhibits the behavior of first decrease and latter increase with the increase of  $q$  for different  $v$ , which was also observed in the study of stationary case [23].

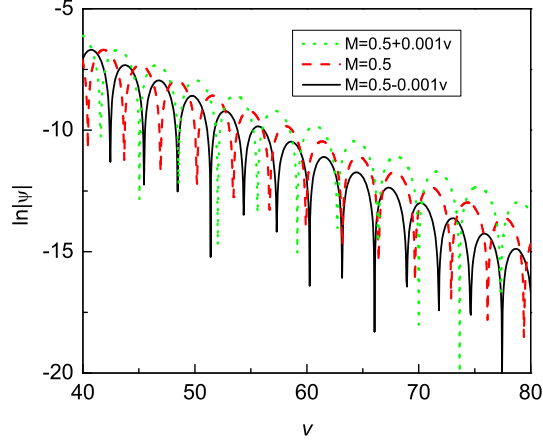


Figure 2: Temporal evolution of the field in the background of Vaidya metric ( $q=0$ ) for  $l = 2$ , evaluated at  $r = 5$ . The mass of the black hole is  $M(v) = 0.5 \pm 0.001v$ . The field evolution for  $M(v) = 0.5 + 0.001v$  and  $M(v) = 0.5 - 0.001v$  are shown as the top curve and the bottom curve respectively. For comparison, the oscillations for  $M = 0.5$  is given in the middle line.

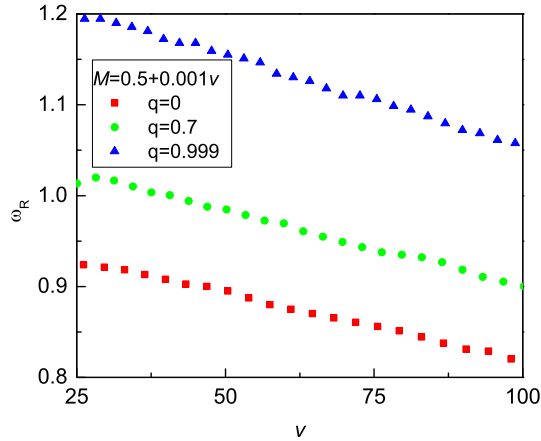


Figure 3: The frequency  $\omega_R$  for  $l = 2$ , evaluated at  $r = 5$  in the linearly absorbing black hole  $M(v) = 0.5 + 0.001v$ .

In order to compare with the QNMs in the stationary RN black hole, we plot the curves  $c_R(l, q)/\omega_R$  and  $c_I(l, q)/\omega_I$  with respect to time  $v$  as shown in Fig.7-10.  $c_R(l, q)$  and  $c_I(l, q)$  are defined in (11). It is interesting to note that all these curves for  $M(v) = 0.5+0.001v$  are nearly equal for different  $q$ . Similar results are obtained for the curves corresponding to  $M(v) = 0.5 - 0.001v$ . The slope of the curve  $c_R(l, q)/\omega_R$  (or  $c_I(l, q)/\omega_I$ ) is equal to the  $\dot{M}$ , which suggests that the

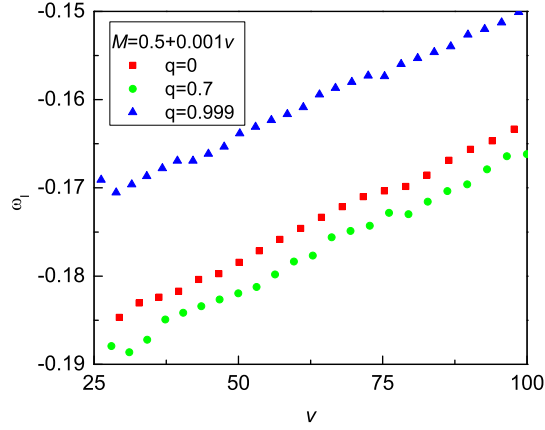


Figure 4: The frequency  $\omega_I$  for  $l = 2$ , evaluated at  $r = 5$  in the linearly absorbing black hole  $M(v) = 0.5 + 0.001v$ .

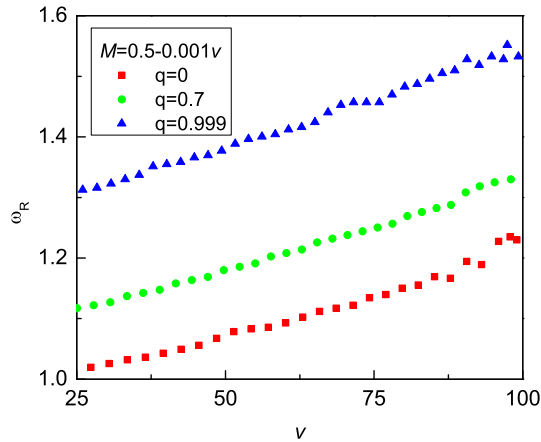


Figure 5: The frequency  $\omega_R$  for  $l = 2$ , evaluated at  $r = 5$  in the linearly evaporating black hole  $M(v) = 0.5 - 0.001v$ .

formula (11) is still a good approximation. In fact we find

$$M(v - v') \approx \frac{c_R(l, q)}{\omega_R(v - v')}, M(v - v') \approx \frac{c_I(l, q)}{\omega_I(v - v')}, \quad (29)$$

where the parameter  $v'$  represents the retarded effect. As shown in Fig.11, the frequencies  $\omega_R$  for different position radius  $r$  with  $l = 2$ ,  $q = 0$  and  $M(v) = 0.5 - 0.001v$  are plotted. Clearly, the temporal evolution of the field  $\Psi(r, v)$  at a radius  $r = 20$  has a retard corresponding to the position  $r = 10$ .

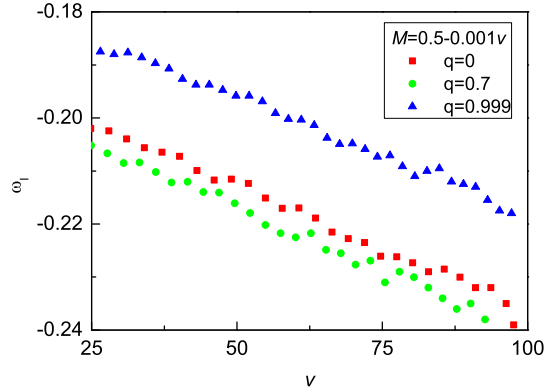


Figure 6: The frequency  $\omega_I$  for  $l = 2$ , evaluated at  $r = 5$  in the linearly evaporating black hole  $M(v) = 0.5 - 0.001v$ .

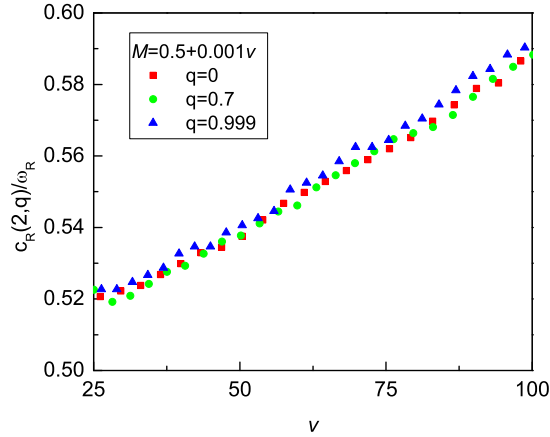


Figure 7:  $c_R(l, q)/\omega_R$  as the function of time  $v$  for  $l = 2$ ,  $r = 5$  and  $M(v) = 0.5 + 0.001v$ .

We have also extended our discussion to the model with exponentially decreasing mass and charge [26],

$$M(v) = \begin{cases} m_0 & v \leq v_0 \\ m_0 \exp(-\alpha v) & v_0 \leq v \leq v_1 \\ m_1 & v \geq v_1 \end{cases} \quad (30)$$

$$Q(v) = qM(v),$$

where  $m_0$ ,  $m_1$ ,  $\alpha$  and  $q$  are constant parameters. Changing the sign before  $\alpha$ , (30) can be used to describe the absorption process. In order to compare the different results between the exponential

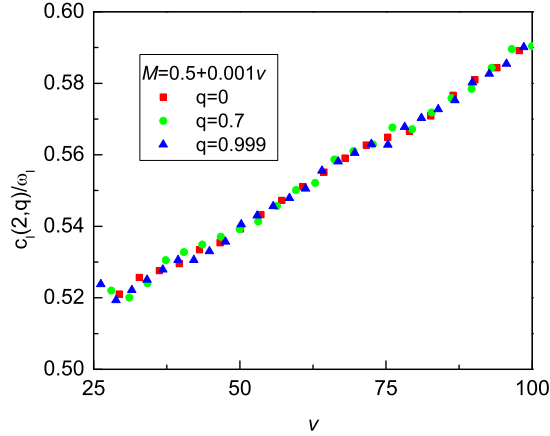


Figure 8:  $c_I(l, q)/\omega_I$  as the function of time  $v$  for  $l = 2$ ,  $r = 5$  and  $M(v) = 0.5 + 0.001v$ .

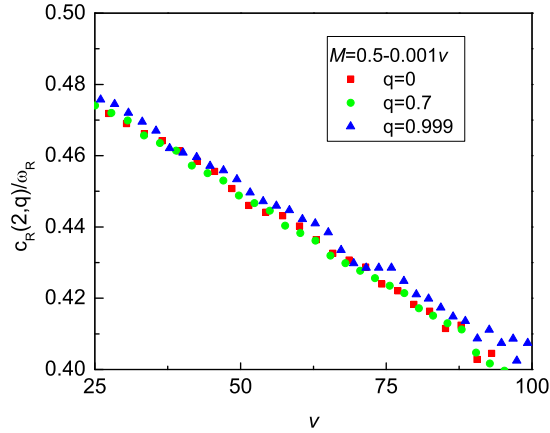


Figure 9:  $c_R(l, q)/\omega_R$  as the function of time  $v$  for  $l = 2$ ,  $r = 5$  and  $M(v) = 0.5 - 0.001v$ .

model and the linear model, we assume that there are two absorbing black holes. The mass of one black hole increases from  $M(v_0) = 0.5$  to  $M(v_1) = 1$  exponentially, while the other increases from  $M(v_0) = 0.5$  to  $M(v_1) = 1$  linearly. Fig.12 shows the  $c_R(l, q)/\omega_R$  and  $c_I(l, q)/\omega_I$  as functions of time  $v$  for the linear and exponential model. The relative parameters in both models are selected as  $l = 2$ ,  $r = 5$ ,  $q = 0.999$ ,  $v_0 = 0$  and  $v_1 = 150$ . The two dot lines are the mass functions  $M(v - v')$  for models (30) and (26) with  $v' = 8$ . In Fig.13 we plotted  $c_R(l, q)/M\omega_R$  and  $c_I(l, q)/M\omega_I$  as a means to check the validity of (29). The behaviors we have observed in Figs. 12, 13 also hold for other values of  $q$  (see Fig. 14 and Fig. 15 for  $q=0$  as an example). In the linear model both  $1/\omega_R$  and  $1/\omega_I$  depend linearly on  $v$ , while in the exponential model both  $1/\omega_R$  and  $1/\omega_I$  depend

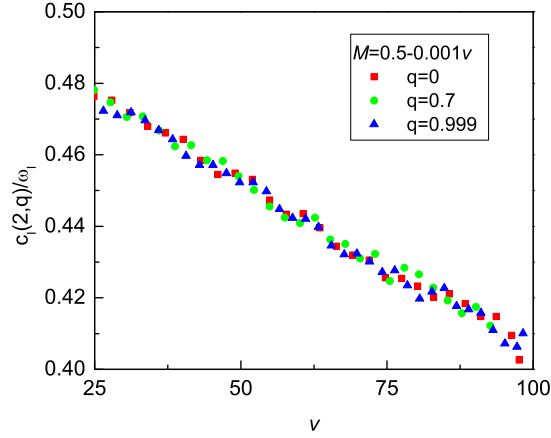


Figure 10:  $c_I(l, q)/\omega_I$  as the function of time  $v$  for  $l = 2$ ,  $r = 5$  and  $M(v) = 0.5 - 0.001v$ .

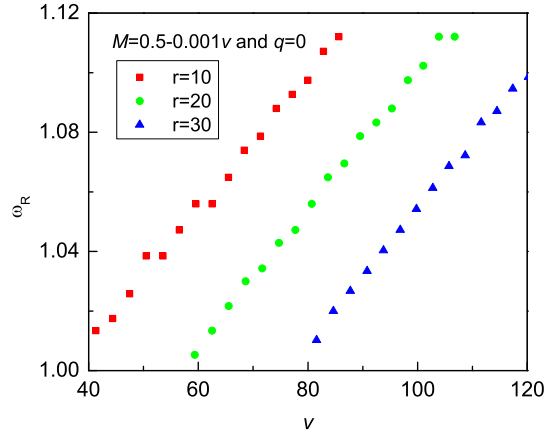


Figure 11:  $\omega_R$  as the function of time  $v$  for  $l = 2$ ,  $q = 0$ ,  $M(v) = 0.5 - 0.001v$ , evaluated at different position  $r = 10$ ,  $r = 20$  and  $r = 30$ . The temporal evolution of the field  $\Psi(r, v)$  at radius  $r = 20$  (or  $r = 30$ ) has a retard to the position  $r = 10$ .

exponentially on  $v$ . The consistency of  $M(v - v')$  and  $c_R(l, q)/\omega_R$  (or  $c_I(l, q)/\omega_I$ ) implies the validity of the equations (29). We have also checked the validity of the equations (29) for different  $l$ , such as  $l = 3, 4, 5$ .

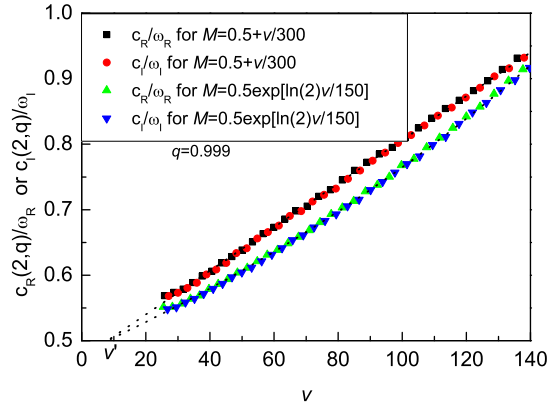


Figure 12:  $c_R(l, q)/\omega_R$  and  $c_I(l, q)/\omega_I$  as the functions of time  $v$  for the linear and exponential model. In the linear model,  $\lambda = -1/150$ , and in the exponential model  $\alpha = -(\ln 2)/150$ . Both models describe the absorption process of the black hole, where the mass increases from  $M(v_0) = 0.5$  to  $M(v_1) = 1$ . The relative parameters in both models are selected as  $l = 2$ ,  $r = 5$ ,  $q = 0.999$ ,  $v_0 = 0$  and  $v_1 = 150$ . The two dot lines are the mass functions  $M(v - v')$  for models (30) and (26) with  $v' = 8$ .

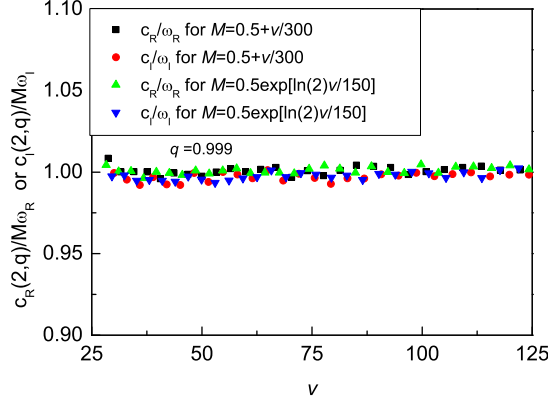


Figure 13:  $c_R(l, q)/M\omega_R$  and  $c_I(l, q)/M\omega_I$  as the functions of time  $v$ . The corresponding parameters are the same as chosen in Fig. 12.

## V. SUMMARY AND DISCUSSION

We have studied the evolution of the massless scalar field propagating in a time-dependent charged Vaidya black hole background. The two generalized tortoise coordinate transformations were used to study the evolution of the massless scalar field. In the first case we used both the  $r_+$  and  $r_-$ , which is appropriated for the case of large charge in numerical calculation. In the other

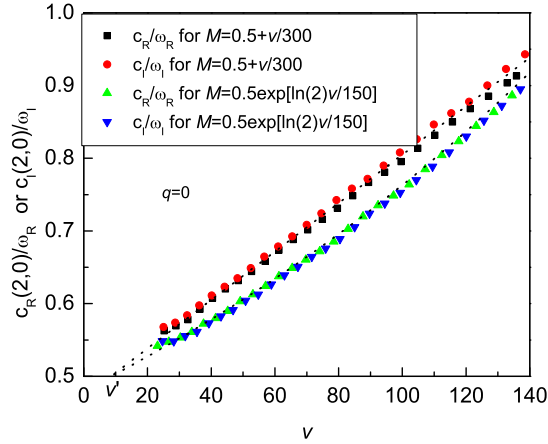


Figure 14:  $c_R(l, q)/\omega_R$  and  $c_I(l, q)/\omega_I$  as the functions of time  $v$  in the case of  $q=0$ . The corresponding parameters are the same as chosen in Fig. 12

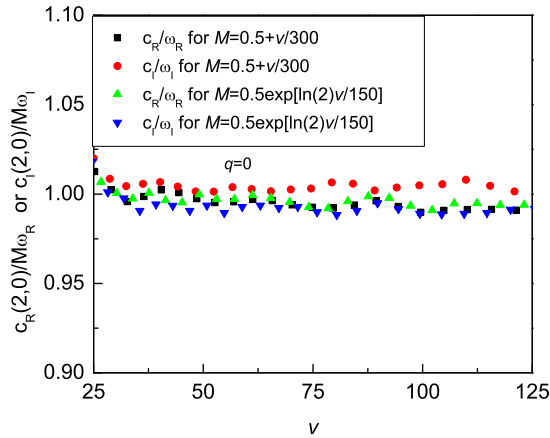


Figure 15:  $c_R(l, q)/M\omega_R$  and  $c_I(l, q)/M\omega_I$  as the functions of time  $v$ . The corresponding parameters are the same as chosen in Fig. 12

case we only used the  $r_+$ , which is appropriated for the case of small charge. The wave equation with a time-dependent scattering potential is derived. In our numerical study, we have found the modification of the QNMs due to the temporal dependence of the black hole spacetimes. In the absorption process, when the black hole becomes bigger, both the imaginary frequency  $|\omega_I|$  and the real frequency  $\omega_R$  decrease with time. However, in the evaporating process, when the black hole loses mass, both  $|\omega_I|$  and  $\omega_R$  increase with the increase of time. The study shows that, for the slowest damped QNMs, the approximate formulas in stationary RN black hole is a good description

for the time-dependent charged Vaidya black hole, which can be expressed as (29).

In general, we conclude that the time dependent processes are well described by an adiabatic approximation with a delay in the definition of the mass function, borrowing the results at each moment from the problem of a black hole of a time-independent masses, instantly equal to the map of the equivalent Vaidya black hole at a retarded time. This implies a huge simplification for the problem of determination of signals from time-dependent processes near black hole. Finally we notice that the period corresponding to QNM is much smaller than the time of flight of a relativistic object in the black hole, actually by several orders of magnitude. We thus conclude that the value we used for the  $\lambda$  parameter is large enough to include realistic cases.

### Acknowledgments

This work was partially supported by NNSF of China, Ministry of Education of China and Shanghai Science and Technology Commission. E. Abdalla's work was partially supported by FAPESP and CNPQ, Brazil. R.K. Su's work was partially supported by the National Basic Research Project of China.

- 
- [1] H.P. Nollert, *Class. Quantum. Grav.* 16, R159 (1999).
  - [2] K.D. Kokkotas and B.G. Schmidt, *Living Rev. Rel.* 2, 2 (1999).
  - [3] P.R. Brady, C.M. Chambers, W. Krivan, and P. Laguna, *Phys. Rev. D* 55, 7538(1997); P.R. Brady, C.M. Chambers, W.G. Laarakkers and E. Poisson, *Phys. Rev. D* 60, 064003 (1999).
  - [4] C. Molina, D. Giugno E. Abdalla and A. Saa, *Phys. Rev. D* 69,104013(2004).
  - [5] D.P. Du, B. Wang and R.K. Su, *Phys. Rev. D* 70,064024(2004); E. Abdalla, B. Wang, A. Lima-Santos and W.G. Qiu, *Phys. Lett. B* 538, 435 (2000); E. Abdalla, K.H.C. Castello-Branco and A. Lima-Santos, *Phys.Rev. D* 66, 104018 (2002)
  - [6] J.S.F. Chan and R.B. Mann, *Phys. Rev. D* 55, 7546 (1997); J.S.F. Chan and R.B. Mann, *Phys. Rev. D* 59, 064025 (1999).
  - [7] V. Cardoso and J.P.S. Lemos, *Phys. Rev. D* 63,124015 (2001).
  - [8] G.T. Horowitz and V.E. Hubeny, *Phys. Rev. D* 62, 024027 (2000).
  - [9] B. Wang, C.Y. Lin and E. Abdalla, *Phys. Lett. B* 481, 79 (2000).
  - [10] B. Wang, C. Molina and E. Abdalla, *Phys. Rev. D* 63, 084001 (2001).
  - [11] V. Cardoso and J.P.S. Lemos, *Phys. Rev. D* 64, 084017 (2001); V. Cardoso and J.P.S. Lemos, *Class. Quantum. Grav.* 18, 5257 (2001).
  - [12] E. Berti and K.D. Kokkotas, *Phys. Rev. D* 67, 064020 (2003).

- [13] R.A. Konoplya, Phys. Rev. D 66, 044009 (2002).
- [14] D. Birmingham, I. Sachs, S.N. Solodukhin, Phys. Rev. Lett. 88, 151301 (2002); D. Birmingham, Phys. Rev. D 64, 064024 (2001).
- [15] J.M. Zhu, B. Wang and E. Abdalla, Phys. Rev. D 63, 124004 (2001); B. Wang, E. Abdalla and R.B. Mann, Phys. Rev. D 65, 084006 (2002); B. Wang, C.Y. Lin and C. Molina, Phys. Rev. D 70, 064025 (2004).
- [16] S. Musiri and G. Siopsis, Phys. Lett. B 576, 309 (2003); R. Aros, C. Martinez, R. Troncoso and J. Zanelli, Phys. Rev. D 67,044014 (2003); A. Nunez and A.O. Starinets, Phys. Rev. D 67,124013 (2003); E. Winstanley, Phys. Rev. D 64,104010 (2001).
- [17] V. Cardoso and J.P.S. Lemos, Phys. Rev. D 67, 084020 (2003); V. Cardoso, R. Konoplya and J.P.S. Lemos, Phys. Rev. D 68, 044024 (2003).
- [18] V. Cardoso, R. Konoplya and J.P.S. Lemos, gr-qc/0305037.
- [19] S. Hod, Phys. Rev. D 66, 024001 (2002)
- [20] L.H. Xue, Z.X. Shen, B. Wang and R.K. Su, Mod. Phys. Lett. A 19, 239(2004).
- [21] V. Suneeta, Phys. Rev. D 68, 024020(2003); F. J. Zerilli, Phys. Rev. D 9, 860 (1974); V. Moncrief, Phys. Rev. D 10, 1057 (1974); D.L. Gunter, Philos. Trans. R. Soc. London, A 296, 497 (1980); K.D. Kokkotas and B.F.Schutz, Phys. Rev. D 37, 3378 (1988); E. W. Leaver, Phys. Rev. D 41, 2986 (1990).
- [22] C. Gundlach, R. H. Price and J. Pullin, Phys. Rev. D 49,883(1994).
- [23] V. Ferrai and B. Mashhoon, Phys. Rev. Lett 52,1361(1984).
- [24] B. Waugh and K. Lake, Phys. Rev. D 34, 2978 (1986).
- [25] Z. Zhao and X. X. Dai, Mod. Phys. Lett. A7, 1771(1992).
- [26] Y. Kaminaga, Class. Quantum. Grav. 7, 1135 (1990); O. Levin and A. Ori, Phys. Rev. D 54,2746 (1996).
- [27] Actually, the event horizon is a global notion in the Vadyia Metric (see [26]). We nevertheless borrow here this terminology.